HELDA
HELSINGIN YLIOPISTO
HELSINGFORS UNIVERSITET
UNIVERSITY OF HELSINKI

UNIVERSITY OF HELSINKI

https://helda.helsinki.fi

Doping dependent plasmon dispersion in 2H-transition metal dichalcogenides

Müller, Eric

2016-07-05

Müller , E , Büchner , B , Habenicht , C , Koenig , A , Knupfer , M , Berger , H & Huotari , S 2016 , ' Doping dependent plasmon dispersion in 2H-transition metal dichalcogenides ' , Physical Review B , vol. 94 , no. 3 , 035110 . https://doi.org/10.1103/PhysRevB.94.035110

http://hdl.handle.net/10138/184155
https://doi.org/10.1103/PhysRevB.94.035110

unspecified
publishedVersion

Downloaded from Helda, University of Helsinki institutional repository.

This is an electronic reprint of the original article.

This reprint may differ from the original in pagination and typographic detail.

Please cite the original version.

Doping dependent plasmon dispersion in 2*H*-transition metal dichalcogenides

Eric Müller,[1] Bernd Büchner,[1] Carsten Habenicht,[1] Andreas König,[1] Martin Knupfer,[1] Helmuth Berger,[2] and Simo Huotari[3]
[1]*IFW Dresden, P.O. Box 270116, D-01171 Dresden, Germany*
[2]*Institut de Physique de la Matière Complexe, EPFL, CH-1015 Lausanne, Switzerland*
[3]*Department of Physics, P.O. Box 64, FI-00014 University of Helsinki, Helsinki, Finland*
(Received 16 March 2016; revised manuscript received 24 May 2016; published 5 July 2016)

We report the behavior of the charge carrier plasmon of 2*H*-transition metal dichalcogenides (TMDs) as a function of intercalation with alkali metals. Intercalation and concurrent doping of the TMD layers have a substantial impact on plasmon energy and dispersion. While the plasmon energy shifts are related to the intercalation level as expected within a simple homogeneous electron gas picture, the plasmon dispersion changes in a peculiar manner independent of the intercalant and the TMD materials. Starting from a negative dispersion, the slope of the plasmon dispersion changes sign and grows monotonously upon doping. Quantitatively, the increase of this slope depends on the orbital character (4*d* or 5*d*) of the conduction bands, which indicates a decisive role of band structure effects on the plasmon behavior.

DOI: 10.1103/PhysRevB.94.035110

I. INTRODUCTION

Layered, quasi-two-dimensional transition-metal dichalcogenides (TMDs) harbor a wealth of fascinating physical phenomena. Their metallic representatives, e.g., $NbSe_2$ or $TaSe_2$, represent ideal systems to study the effects of dimensionality, doping, or external fields on correlated electronic phases, for instance, charge density waves (CDW), superconductivity, or orbital order phenomena [1–7]. Many of the transition-metal dichalcogenides with a metallic ground state are considered to be prototype CDW materials. Often, as in 2*H*-$NbSe_2$ or 2*H*-$TaSe_2$, the phase transition into the charge ordered state gives rise to a pseudogap at the Fermi level [8] and at lower temperatures superconductivity appears [5]. Then, these two phases seem to coexist. The microscopic origin of these phenomena, however, still is under debate.

As a consequence of their metallic ground state, these materials can also host collective density oscillations of the charge carriers, so-called plasmons, in addition to the single-particle excitations [9,10]. The energy required to excite such collective plasmon modes is given by the plasma frequency $\omega_p^2 = ne^2/\epsilon_0 m$, which scales with the density n of the conduction electrons and easily reaches several eV for ordinary metals (e denotes the elementary charge, m the electron effective mass, and ϵ_0 the free space permittivity). Furthermore, these plasmons are characterized by a particular momentum (q) dependence. For a simple metal in the long wavelength limit, the plasmon dispersion is expected to be quadratic [9,10],

$$\omega_p(\mathbf{q}) = \omega_p(0) + \frac{3}{10}\frac{v_F^2}{\omega_p(0)}q^2. \quad (1)$$

Thereby, v_F and m denote the (averaged) Fermi velocity and the electron mass, respectively. Thus the plasmon dispersion and its anisotropy harbors information about the Fermi surface. We note that a positive quadratic plasmon dispersion has been observed in many systems, among them also correlated electron systems, and it has been used to achieve Fermi surface shape and anisotropy in some systems [11–14].

However, the TMD materials revealed an unexpected behavior beyond the simple equation shown above. The momentum dependence of the charge carrier plasmon was observed to be negative, i.e., the plasmon energy shifted to lower energies with increasing momentum transfer [15,16]. This surprising observation has been discussed on the basis of different contributions. For instance, it has been proposed that charge density wave instabilities (below the corresponding phase transition) and fluctuations (above the phase transition) in those compounds can cause a negative plasmon dispersion via their interaction with the plasmon oscillations. This could be modeled within a semiclassical Ginzburg-Landau description [16]. On the other hand, band structure calculations of these compounds have indicated that the negative plasmon dispersion can be attributed to the particular behavior of the intraband transitions within the conduction bands that give rise to the plasmon [17,18]. Moreover, interband transitions may give additional momentum-dependent screening contributions which also can alter the plasmon dispersion substantially. Particular variants of the plasmon dispersion due to contributions from interband transitions have, for instance, been observed in heavier alkali metals [19–21] and alkali intercalated C_{60} [22].

In addition, it has also been demonstrated that upon intercalation of 2*H*-$TaSe_2$ with potassium the plasmon dispersion changes sign to positive values. At the same time the charge density wave is suppressed with this intercalation and the concomitant electron transfer to (i.e., doping of) the layers [23,24].

In order to complement our knowledge on the plasmon dispersion in various metallic TMDs and its variation due to doping, we extended the previous work significantly via the investigation of the plasmon dispersion in K_xTaS_2, Na_xTaSe_2, K_xNbSe_2, and Na_xNbSe_2 using electron energy-loss spectroscopy (EELS) in transmission. This is the method of choice for the investigation of the momentum dependence of different excitations in solids [11,16,25,26]. Our results demonstrate that in all investigated TMD compounds, the plasmon dispersion monotonously increases upon charge transfer to the TMD layers, indicating a universal behavior for these materials. Moreover, the observed doping dependent variations indicate a different behavior for the Nb-based compounds with 4*d*-derived conduction bands as compared to Ta-based

 ©2016 American Physical Society

compounds with 5*d*-derived bands, which demonstrates the importance of band structure effects.

II. EXPERIMENT

Thin films of metallic transition metal dichalcogenides were prepared by exfoliation of the respective single crystals. These crystals were grown by thermal gradient using iodine as a transport agent ($TaSe_2$, $NbSe_2$) [24,27] or commercially available (TaS_2, NbS_2) [28], respectively. To obtain films with a thickness of about 100 nm, the single crystals were cleaved repeatedly with adhesive tape. These films were then mounted onto standard electron microscopy grids and transferred into the spectrometer, where we investigated the electronic excitation spectrum using electron energy-loss spectroscopy in transmission. Previously, this procedure had already been applied successfully to TMD materials [15].

All electron energy-loss measurements were carried out using the 172 keV spectrometer described in detail elsewhere [29,30]. The energy and momentum resolution were chosen to be 82 meV and 0.04 $Å^{-1}$ at room temperature. EELS probes the loss function $\mathrm{Im}[-1/\epsilon(\mathbf{q},\omega)]$, which is proportional to the dynamic structure factor $S(\mathbf{q},\omega)$, for a momentum transfer $\mathbf{q}$ parallel to the film surface [$\epsilon(\mathbf{q},\omega)$ is the dielectric function]. Prior to the inelastic measurements on pristine samples, all films have been characterized using *in situ* electron diffraction. These diffraction data confirmed the high crystallinity of the films in all cases (see previous publications for details: Refs. [15,23]).

The samples were intercalated with sodium and potassium by thermal evaporation from commercial SAES (SAES GETTERS S.P.A., Italy) alkali metal dispensers under ultrahigh vacuum conditions (base pressure below 10^{-10} mbar). Intercalation was performed stepwise in discrete intervals of 3 min. To assure a homogeneous distribution of the dopant, the samples were annealed for 1 h at a temperature of 100 °C after each doping step. Our previous investigations demonstrated that homogeneously intercalated films can be achieved in this way [23,24]. In order to analyze the doping (intercalation) level, we estimated the charge that is transferred to the dichalcogenide layers following the procedure of Campagnoli *et al.* [31]. This is based on the Drude model, and the doping level x is calculated by

$$x = 1 - \frac{\omega_P^2}{\omega_0^2}, \tag{2}$$

with ω_P and ω_0 being the plasmon position of the actual doped and pure sample, respectively.

This procedure takes into account that intercalation with alkali metals results in a doping of the dichalcogenides, which directly causes a reduction of the plasmon energy (see below). Starting from half-filled conduction bands in, e.g., undoped $2H$-$NbSe_2$, the addition of electrons is expected to lower the plasmon energy following the equation above within a rigid band consideration [31], which can be rationalized considering holes instead of electrons as usually done for hole-doped semiconductors. Thus an analysis of the energy positions of the charge carrier plasmons (see Fig. 2 below) directly provides us with the doping level, and we use the doping levels obtained in this way throughout the rest of this paper. We note that recent band structure calculations of potassium intercalated $TaSe_2$ have confirmed the results from such an analysis [23].

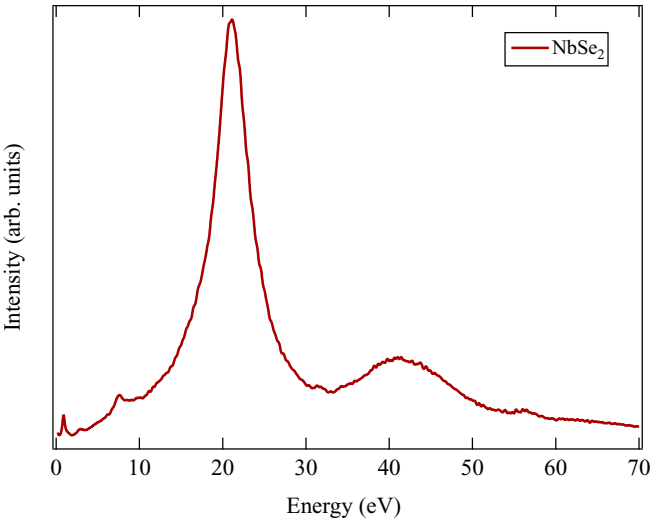

FIG. 1. Electron energy-loss spectrum of $2H$-$NbSe_2$.

III. RESULTS AND DISCUSSION

To illustrate the information that is obtained using EELS, we depict in Fig. 1 the energy-loss spectrum of pure $2H$-$NbSe_2$ for an energy range up to 70 eV. The distinctive feature around 21 eV represents the collective excitation of all valence electrons, the so-called volume plasmon. At higher energies shallow core level excitations from Nb 4*p* (around 31 and 32 eV), and from Se 3*d* (around 55 eV) contribute to the spectra. Moreover, multiple scattering contributions can occur around 42 eV. At about 1 eV there appears a well defined, relatively sharp feature which is due to the charge-carrier plasmon. This represents the collective excitation of all the conduction electrons and it is this feature we want to focus on in the following. The overall EELS spectra for other $2H$-TMD compounds are very similar to what is seen in Fig. 1 [15,32].

Figure 2 concentrates on the energy region of the charge carrier plasmon of intercalated $2H$-Na_xNbSe_2 and $2H$-K_xNbSe_2. The depicted spectra were normalized between 4 and 5 eV. Undoped $2H$-$NbSe_2$ is characterized by a charge carrier plasmon centered around 0.9 eV. Upon doping with potassium or sodium, the plasmon energy continuously shifts to smaller values, as seen in Fig. 2. The corresponding energy values have been used to analyze the doping level as discussed in the previous section. The behavior observed for $2H$-Na_xNbSe_2 and $2H$-K_xNbSe_2 parallels that for $2H$-K_xTaSe_2 published previously [23,24]. Moreover, Fig. 2 reveals a concomitant continuous decrease of the spectral width of the plasmon features upon rising doping level. This continuous decrease of plasmon position and width strongly indicates a homogeneous distribution of the potassium and sodium ions in all intercalated $2H$-$NbSe_2$ samples, since the formation of stable intercalated phases with well defined composition would lead to a superposition of the respective spectral information and the appearance of double peak or broadened features for intercalation levels in between the stable stoichiometries. Again, the data and

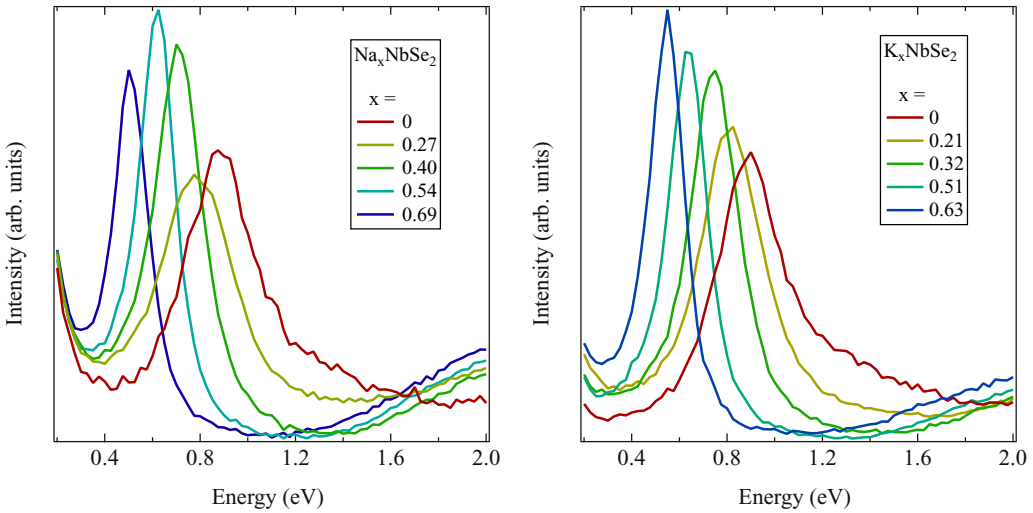

FIG. 2. Evolution of the charge carrier plasmon in 2H-$NbSe_2$ as a function of doping with Na and K, respectively.

this conclusion agree well with what has been observed for potassium doped 2H-$TaSe_2$ [23,24].

Previous work on the dispersion of the charge carrier plasmon in 2H-$TaSe_2$, 2H-$NbSe_2$, and 2H-TaS_2 has demonstrated that the plasmons disperse negatively, which is in contrast to the expectation for the free electron gas and the observation in many other metallic systems [15,16]. Further experiments have shown that upon intercalation with potassium and the induced charging of 2H-$TaSe_2$ the plasmon dispersion changes dramatically, becoming positive with increasing slopes upon growing intercalation level [24]. We have extended this work to intercalation with sodium and intercalating other dichalcogenides. In Fig. 3, we show the behavior of the charge carrier plasmon in undoped 2H-$NbSe_2$ as well as for a selected value of potassium ($x = 0.63$) and sodium ($x = 0.69$) intercalation as a function of momentum transfer. The negative plasmon dispersion for the undoped case is nicely confirmed. In very good agreement with the above mentioned potassium intercalated 2H-$TaSe_2$, the plasmon dispersion becomes clearly positive for both potassium and sodium intercalation of 2H-$NbSe_2$.

The evolution of the plasmon dispersion in 2H-$NbSe_2$ as a function of potassium and sodium intercalation is summarized in Fig. 4. It becomes clear that the plasmon dispersion continuously increases with growing intercalation level, i.e., with increasing electron addition to the dichalcogenide layers. For a more quantitative analysis of these data we followed Ref. [24] and fitted the plasmon dispersion using a linear dependence up to 0.3 $Å^{-1}$. Such a linear description fits the measured data very well, although a linear plasmon dispersion is beyond the expectations for simple electron systems [9,10]. Thus such a linear fit allows one to determine the slope of the plasmon dispersion in a momentum range of 0.1 $Å^{-1}$ to 0.3 $Å^{-1}$ in a reasonable manner. As already mentioned, this had already been done for K_xTaSe_2, and we have carried out equivalent experiments and analyses for Na_xTaSe_2 and Na_xTaS_2. In Fig. 5 we compare all available results on the behavior of the plasmon dispersion as a function of doping of 2H-$TaSe_2$, 2H-TaS_2, and 2H-$NbSe_2$ with the alkali metals potassium and sodium. Additionally included is the dispersion of a $Nb_{1+x}S_2$ sample, where doping is provided by excess Nb and where the doping level has been analyzed as described above.

Our data show that for all combinations of alkali metal and dichalcogenide the slope of the plasmon dispersion

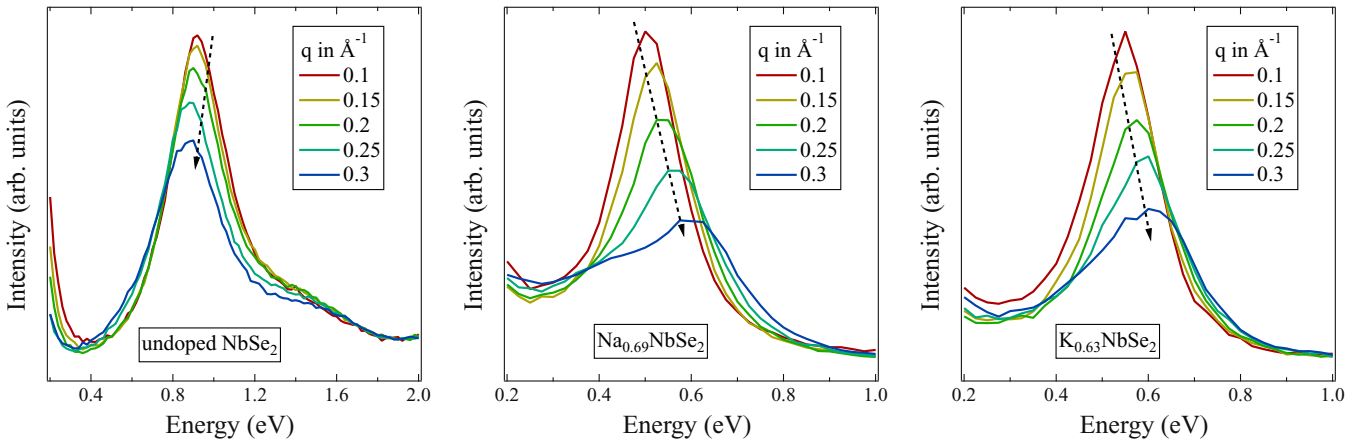

FIG. 3. Dispersion of the charge carrier plasmon in undoped as well as selected Na- and K-doped 2H-$NbSe_2$, respectively.

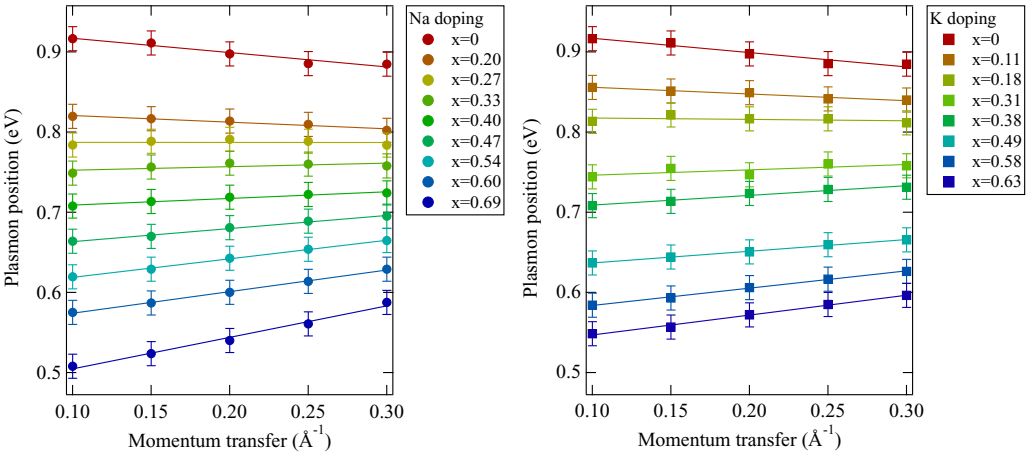

FIG. 4. Doping dependence of the plasmon dispersion in Na- and K-doped 2H-$NbSe_2$. The data have been obtained by analyzing the energy position of the plasmon maxima; for a selection see Fig. 3 (for details see text).

continuously increases with increasing doping level. Always starting from a negative value, it becomes positive around a doping level x of about 0.15 to 0.25. As mentioned above, there have been alternative suggestions how to rationalize the negative plasmon dispersion in the undoped compounds. It would be interesting to see whether these models would also be able to describe the doping dependent variations of the plasmon dispersion.

It has been shown that upon doping of the order of 15% or less the charge density wave formation in 2H-TMDC systems can be weakened substantially or even completely suppressed [23,33,34]. It is thus tempting to place the changes of the plasmon dispersion into this context. Recalling the already mentioned semiclassical Ginzburg-Landau approach, where the negative plasmon dispersion has been associated with an interaction between charge density fluctuations and the plasmon resonance [16], this kind of renormalization of the plasmon dispersion naturally should become weaker or even disappear upon doping in parallel with the charge density wave suppression. However, within this framework, it remains unclear why the slope of plasmon dispersion monotonously increases upon doping even far above the CDW suppression. For a homogeneous electron gas, one would actually expect the plasmon dispersion to become smaller with decreasing plasmon energy at vanishing momentum [10].

Alternatively, the negative plasmon dispersion in the undoped transition metal dichalcogenides has been ascribed to the particular band structure and the related possible transitions within the conduction bands with 4d or 5d character. Then, it is also clear that doping electrons into these bands and shifting the Fermi level accordingly will have an impact on the plasmon behavior. Indeed, shifting the Fermi level in such calculations to simulate a doping effect results in a positive plasmon dispersion for high doping levels in very good agreement to the experimental data [17,35]. Therefore, our data more support the picture that the particular band structure in the 2H-TMD systems is responsible for the peculiar behavior of the plasmon dispersion.

Figure 5 reveals another interesting aspect. The data for the varying slopes of the plasmon dispersion fall into two categories. They are significantly different for the Nb based compounds as compared to those containing Ta. In other words, the doping induced variation of the plasmon dispersion depends on the orbital character of the conduction bands; it is different for compounds in which the conduction band is made up of 4d or 5d states, respectively. This observation also nicely fits to our conclusion that the conduction bands and their detailed structure are important to understand the plasmons and their dispersion.

IV. SUMMARY

We have presented electron energy-loss spectroscopy studies of various 2H-transition metal dichalcogenides that were intercalated using the alkali metals potassium and sodium. We have shown that in all cases this intercalation and the induced

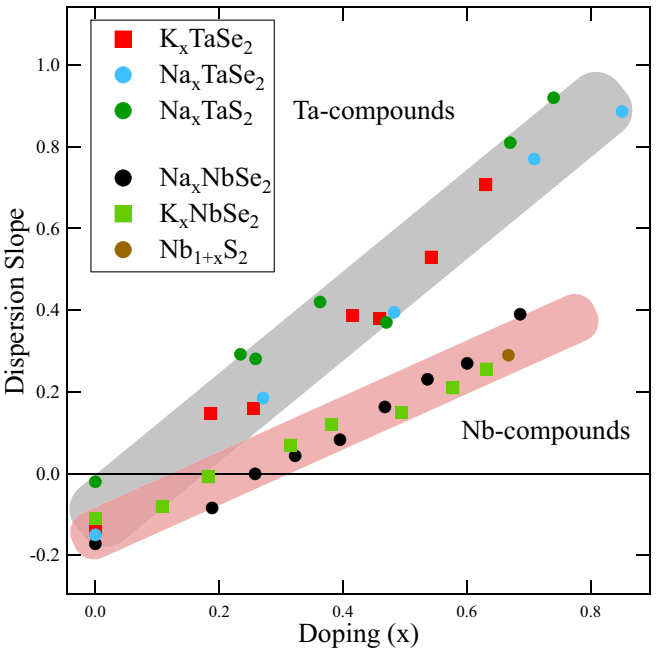

FIG. 5. Comparison of the slope of the charge carrier plasmon dispersion as a function of doping for Ta- and Nb-based 2H-transition metal dichalcogenides.

charge transfer to the dichalcogenide layers have a dramatic effect on the plasmon energy and dispersion. The plasmon energy shifts to lower values with increasing intercalation, a behavior that is expected as a consequence of the filling of the conduction bands with electrons. We have used this shift in order to analyze the corresponding doping level, respectively.

The plasmon dispersion, being initially negative, changes sign and increases further with increasing doping level. Moreover, there is strong indication that this increase depends on the orbital character of the conduction bands; it is larger for the 5*d* (Ta-based) compounds than in case of the 4*d* (Nb-based) materials. This suggests a particular role of the conduction bands in the determination of the plasmon dispersion, which supports explanations of the peculiar plasmon behavior in undoped and doped dichalcogenides in the framework of the particular band structure of these materials.

ACKNOWLEDGMENTS

We thank M. Naumann, R. Hübel, and S. Leger for their technical assistance. S.H. was supported by the Academy of Finland (Projects No. 1254065, No. 1283136, and No. 1259526).

[1] J. A. Wilson and A. D. Yoffe, Adv. Phys. **18**, 193 (1969).
[2] J. A. Wilson, F. J. D. Salvo, and S. Mahajan, Adv. Phys. **24**, 117 (1975).
[3] E. A. Marseglia, Int. Rev. Phys. Chem. **3**, 177 (1983).
[4] R. H. Friend and A. D. Yoffe, Adv. Phys. **36**, 1 (1987).
[5] A. H. Castro Neto, Phys. Rev. Lett. **86**, 4382 (2001).
[6] H. Cercellier, C. Monney, F. Clerc, C. Battaglia, L. Despont, M. G. Garnier, H. Beck, P. Aebi, L. Patthey, H. Berger, and L. Forró, Phys. Rev. Lett. **99**, 146403 (2007).
[7] T. Ritschel, J. Trinckauf, K. Koepernik, B. Büchner, M. v. Zimmermann, H. Berger, Y. I. Joe, P. Abbamonte, and J. Geck, Nat. Phys. **11**, 328 (2015).
[8] S. V. Borisenko, A. A. Kordyuk, A. N. Yaresko, V. B. Zabolotnyy, D. S. Inosov, R. Schuster, B. Büchner, R. Weber, R. Follath, L. Patthey, and H. Berger, Phys. Rev. Lett. **100**, 196402 (2008).
[9] P. Nozières and D. Pines, Phys. Rev. **113**, 1254 (1959).
[10] W. Nolting, *Grundkurs Theoretische Physik 7*, 8th ed. (Springer, Spektrum, 2015).
[11] N. Nücker, U. Eckern, J. Fink, and P. Müller, Phys. Rev. B **44**, 7155 (1991).
[12] V. G. Grigoryan, G. Paasch, and S.-L. Drechsler, Phys. Rev. B **60**, 1340 (1999).
[13] S. Huotari, M. Cazzaniga, H.-C. Weissker, T. Pylkkänen, H. Müller, L. Reining, G. Onida, and G. Monaco, Phys. Rev. B **84**, 075108 (2011).
[14] M. Cazzaniga, H.-C. Weissker, S. Huotari, T. Pylkkänen, P. Salvestrini, G. Monaco, G. Onida, and L. Reining, Phys. Rev. B **84**, 075109 (2011).
[15] R. Schuster, R. Kraus, M. Knupfer, H. Berger, and B. Büchner, Phys. Rev. B **79**, 045134 (2009).
[16] J. van Wezel, R. Schuster, A. König, M. Knupfer, J. van den Brink, H. Berger, and B. Büchner, Phys. Rev. Lett. **107**, 176404 (2011).
[17] P. Cudazzo, M. Gatti, and A. Rubio, Phys. Rev. B **86**, 075121 (2012).
[18] M. N. Faraggi, A. Arnau, and V. M. Silkin, Phys. Rev. B **86**, 035115 (2012).
[19] A. vom Felde, J. Sprösser-Prou, and J. Fink, Phys. Rev. B **40**, 10181 (1989).
[20] F. Aryasetiawan and K. Karlsson, Phys. Rev. Lett. **73**, 1679 (1994).
[21] K. Kimura, K. Matsuda, N. Hiraoka, Y. Kajihara, T. Miyatake, Y. Ishiguro, T. Hagiya, M. Inui, and M. Yao, J. Phys. Soc. Jpn. **84**, 084701 (2015).
[22] O. Gunnarsson, V. Eyert, M. Knupfer, J. Fink, and J. F. Armbruster, J. Phys.: Condens. Matter **8**, 2557 (1996).
[23] A. König, K. Koepernik, R. Schuster, R. Kraus, M. Knupfer, B. Büchner, and H. Berger, Europhys. Lett. **100**, 27002 (2012).
[24] A. König, R. Schuster, M. Knupfer, B. Büchner, and H. Berger, Phys. Rev. B **87**, 195119 (2013).
[25] M. Knupfer, T. Pichler, M. S. Golden, J. Fink, M. Murgia, R. H. Michel, R. Zamboni, and C. Taliani, Phys. Rev. Lett. **83**, 1443 (1999).
[26] R. Schuster, J. Trinckauf, C. Habenicht, M. Knupfer, and B. Büchner, Phys. Rev. Lett. **115**, 026404 (2015).
[27] F. Lévy and H. Berger, J. Cryst. Growth **61**, 61 (1983).
[28] http://www.2dsemiconductors.com.
[29] J. Fink, in *Recent Developments in Energy-Loss Spectroscopy*, edited by P. W. Hawkes, Advances in Electronics and Electron Physics Vol. 75 (Academic Press, New York, 1989), pp. 121–232.
[30] F. Roth, A. König, J. Fink, B. Büchner, and M. Knupfer, J. Electron Spectrosc. Relat. Phenom. **195**, 85 (2014).
[31] G. Campagnoli, A. Gustinetti, A. Stella, and E. Tosatti, Phys. Rev. B **20**, 2217 (1979).
[32] M. Bell and W. Liang, Adv. Phys. **25**, 53 (1976).
[33] L. Fang, Y. Wang, P. Y. Zou, L. Tang, Z. Xu, H. Chen, C. Dong, L. Shan, and H. H. Wen, Phys. Rev. B **72**, 014534 (2005).
[34] D. W. Shen, B. P. Xie, J. F. Zhao, L. X. Yang, L. Fang, J. Shi, R. H. He, D. H. Lu, H. H. Wen, and D. L. Feng, Phys. Rev. Lett. **99**, 216404 (2007).
[35] P. Cudazzo, E. Müller, C. Habenicht, M. Gatti, H. Berger, M. Knupfer, A. Rubio, and S. Huotari, arXiv:1603.03486v1.